

Counterfactual Explanations for Hypergraph Neural Networks

Fabiano Veglianti¹ Lorenzo Antonelli¹ Gabriele Tolomei²

Abstract

Hypergraph neural networks (HGNNS) effectively model higher-order interactions in many real-world systems but remain difficult to interpret, limiting their deployment in high-stakes settings.

We introduce CF-HyperGNNEExplainer, a counterfactual explanation method for HGNNS that identifies the minimal structural changes required to alter a model’s prediction. The method generates counterfactual hypergraphs using actionable edits limited to removing node-hyperedge incidences or deleting hyperedges, producing concise and structurally meaningful explanations. Experiments on three benchmark datasets show that CF-HyperGNNEExplainer generates valid and concise counterfactuals, highlighting the higher-order relations most critical to HGNN decisions.

1. Introduction

Many real-world systems are governed by higher-order interactions (HOIs), in which outcomes depend on groups of entities rather than on pairwise relations alone. Examples include co-authorship teams, biochemical complexes, group communications, and multi-item user sessions, where the joint context of three or more units carries information that cannot be faithfully reduced to binary links without loss or distortion. Recent work on “networks beyond pairwise interactions” (Battiston et al., 2020) has shown that explicitly modeling HOIs can substantially improve the ability to characterize structure, learn representations, and predict dynamical behavior in complex systems. Consequently, there is increasing interest in learning frameworks that can natively encode group interactions instead of approximating them via pairwise expansions.

Hypergraphs provide a principled representation for HOIs by allowing a hyperedge to connect an arbitrary number

¹Department of Computer Control and Management Engineering, Sapienza University, Rome, Italy ²Department of Computer Science, Sapienza University, Rome, Italy. Correspondence to: Fabiano Veglianti <veglianti@diag.uniroma1.it>.

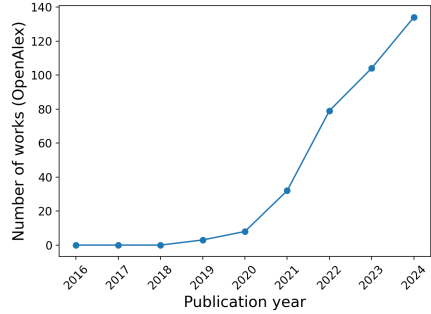


Figure 1. Temporal evolution of publications containing the exact phrase “hypergraph neural network”.

of nodes. Classical hypergraph learning demonstrated that hypergraphs can represent complex relationships more completely than graphs for tasks such as clustering, classification, and embedding (Zhou et al., 2006). Building on this foundation, hypergraph neural networks (HGNNS) (Feng et al., 2019) and hypergraph convolutional neural networks (HGCNs) (Yadati et al., 2019) have emerged as deep learning paradigms that extend graph neural networks and graph convolutional networks to hypergraph-structured data, respectively. Reflecting this momentum, recent surveys synthesize a rapidly expanding body of deep learning on hypergraphs, exploring architectures, training strategies, and applications (Kim et al., 2024). In line with these developments, our bibliometric analysis in Figure 1 shows a clear upward trend in the number of publications on hypergraph neural networks, supporting the view that HGNNS are an emerging and fast-growing modeling tool. Although powerful, HGNNS suffer from limited interpretability, which reduces user trust and constrains their deployment in high-stakes settings. Among eXplainable AI (XAI) approaches proposed in the literature, counterfactual (CF) explanations have attracted growing attention, as they describe minimal changes to an input that would lead to a different model outcome. In the graph domain, this motivation has driven substantial progress in graph neural networks (GNNs) explainability, ranging from post-hoc explainers that highlight predictive substructures (e.g., GNNExplainer (Ying et al., 2019) and PGExplainer (Luo et al., 2020)) to methods that explicitly generate counterfactual graphs (e.g., CF-GNNExplainer (Lucic et al., 2022) and RCEExplainer (Bajaj et al., 2022)). However, transferring these ideas to hyper-

graphs is non-trivial: hyperedges encode higher-order relations whose combinatorial structure and semantics cannot be reduced to pairwise links without altering the meaning of the interactions. Consequently, hypergraph explainability has received comparatively limited attention. Dedicated hypergraph explainers have only emerged recently (e.g., HyperEX (Maleki et al.) and SHyP (Su et al., 2024)), underscoring both the nascent of the area and the open need for explanation tools tailored to hypergraph learning.

In this work, we introduce CF-HyperGNExplainer, the first counterfactual explanation technique specifically designed for hypergraph neural networks. Our goal is to produce valid and interpretable counterfactuals that respect the discrete, higher-order nature of hypergraphs – e.g., by minimally editing hyperedge memberships or hyperedge existence while altering model prediction. This formulation yields explanations that answer questions of the form: “Which higher-order interactions must be removed, or rewired for the HGNN to change its decision?”, thereby directly exposing the role of HOIs in the model’s reasoning.

Our main contributions are as follows: (1) we introduce CF-HyperGNExplainer, the first counterfactual explanation method tailored to HGNNs, generating actionable counterfactual hypergraphs via minimal structural edits; (2) we propose two variants that operate at different granularities, i.e., removing node-hyperedge incidences (NHP) or deleting entire hyperedges (HP); (3) we provide an extensive empirical evaluation on three citation-network datasets, including comparisons with graph-based counterfactual explainers, an ablation study, and a runtime analysis showing that our method strongly outperforms graph-based baseline methods when adapted to native hypergraph settings.

2. Related Work

The body of work most relevant to our study comprises research on hypergraph neural network explainability (Section 2.1) and counterfactual explanations (Section 2.2).

2.1. Hypergraph Neural Network Explainability

Despite the rapid progress in HGNNs, explainability for hypergraph-based classifiers has only recently started to receive dedicated attention. Existing approaches largely extend the intuition of subgraph-based explanations to the hypergraph setting, aiming to identify sub-hypergraphs or node-hyperedge attributions that drive a prediction. HyperEX (Maleki et al.) is a post-hoc framework that scores the importance of node-hyperedge pairs and extracts explanatory sub-hypergraphs for HGNN predictions. SHyP (Su et al., 2024) is a model-agnostic explainer that discretely samples explanation sub-hypergraphs for local attribution, and additionally derives global concepts through

unsupervised extraction. For intrinsically interpretable designs, SHy (Yu et al., 2025) introduces a self-explaining HGNN for electronic health records based diagnosis prediction, producing distinct patient-specific temporal phenotypes as personalized explanations. Finally, models can embed interpretability into their architecture; for instance, Bi et al. (an Bi et al., 2023) propose an explainable and programmable hypergraph convolutional network for imaging-genetics fusion that links decisions to hypergraph components and programmable constraints.

2.2. Counterfactual Explanations

Counterfactual explanations have emerged as a prominent class of instance-based explanations for AI/ML model predictions. Formally, given a classifier f and an input x for which $f(x) = y$, a counterfactual explanation is a perturbed version of the input x' , such that $f(x') = y'$ (where $y' \neq y$) and the difference between x and x' is minimized according to some distance metric (Wachter et al., 2017).

In the context of graph-structured data, CFs aim to answer: “How should the graph structure or node features be minimally modified to change the model’s prediction?”. RC-Explainer (Bajaj et al., 2022) generates robust counterfactual explanations by identifying a small set of important edges within a node n-hop neighborhood such that deleting those edges flips the prediction, with the robustness coming from modeling decision boundaries that covers many training instances with the same predicted class. Differently, CF-GNExplainer (Lucic et al., 2022) formulates counterfactual generation as an optimization problem over the graph structure, seeking the minimal perturbation to the adjacency matrix that induces a change in the model’s prediction for a given target node. A key contribution of CF-GNExplainer is its explicit focus on structural counterfactuals, emphasizing edge deletions as the primary explanation mechanism, while keeping node features fixed. This formulation enables model-agnostic applicability to a wide range of message-passing GNN architectures and provides intuitive explanations in terms of graph edits. However, the method is inherently designed for pairwise relational data represented by adjacency matrices. As a result, CF-GNExplainer cannot be directly extended to HGNNs, where higher-order relationships are encoded through incidence structures and hyperedges connecting arbitrary-sized node sets. This limitation is addressed in our work where we develop a counterfactual explanation method tailored specifically to the hypergraph setting.

3. Background

Our approach builds on the core idea behind CF-GNExplainer (Lucic et al., 2022): generate counterfactual explanations by searching for the smallest structural edit

to the input relational structure that flips a trained model’s prediction. For this reason, in this section we review CF-GNNExplainer, to clarify the counterfactual optimization template we inherit, and the hypergraph neural network propagation operator, to make explicit where and how structural edits can be injected in a differentiable manner.

3.1. Notation

Vectors are bold lowercase (e.g., $\mathbf{x}, \mathbf{y} \in \mathbb{R}^d$). Matrices are uppercase roman (e.g., $A, B \in \mathbb{R}^{n \times m}$). The (i, j) -th entry of A is A_{ij} . The i -th row of A is $A_{i \cdot} \in \mathbb{R}^{1 \times m}$ and the j -th column is $A_{\cdot j} \in \mathbb{R}^{n \times 1}$. The identity matrix is I_d , the all-zeros vector is $\mathbf{0}$, and the all-ones vector is $\mathbf{1}$.

3.2. CF-GNNExplainer

Given a target node v and its k -hop computational subgraph $G_v = (A, X)$, where A is the adjacency matrix and X the feature matrix, the method search for a perturbation matrix P that minimizes the following objective function:

$$\mathcal{L} = -\mathcal{L}_{pred}(f(A \odot P, X), \hat{y}) + \beta \mathcal{L}_{dist}(P)$$

Here, \odot denotes the element-wise product, hence $A \odot P$ is the counterfactual adjacency matrix. The first term, \mathcal{L}_{pred} , encourages the model to flip the prediction from the original prediction y . The second term, \mathcal{L}_{dist} , acts as a regularizer to ensure that the resulting counterfactual remains “close” to the original graph. To handle the discrete nature of edges, P is typically relaxed to continuous values during optimization and thresholded afterward to produce a binary graph structure.

We inherit from CF-GNNExplainer the underlying idea, however, we adapt it to HGNNs. Since CF-GNNExplainer cannot be trivially generalized to HGNNs, we end up with two different algorithm to produce HGNNs’ counterfactual explanations detailed in Section 4.

3.3. Hypergraph Neural Network

Let $G = (V, E)$ be a hypergraph with $|V| = N$ nodes and $|E| = M$ hyperedges. Each hyperedge $\varepsilon \in E$ has an associated positive weight $W_{\varepsilon\varepsilon}$, and all hyperedge weights are stored in the diagonal matrix $W \in \mathbb{R}^{M \times M}$. Unlike simple graphs, a hypergraph is commonly represented by its incidence matrix $H \in \mathbb{R}^{N \times M}$, where

$$H_{i\varepsilon} = \begin{cases} 1, & \text{if } v_i \in V \text{ is incident to hyperedge } \varepsilon \in E, \\ 0, & \text{otherwise.} \end{cases}$$

The node degree matrix $D \in \mathbb{R}^{N \times N}$ and the hyperedge degree matrix $B \in \mathbb{R}^{M \times M}$ are diagonal matrices defined by

$$D_{ii} = \sum_{\varepsilon=1}^M W_{\varepsilon\varepsilon} H_{i\varepsilon}, \quad B_{\varepsilon\varepsilon} = \sum_{i=1}^N H_{i\varepsilon}. \quad (1)$$

Convolution on Hypergraphs. Information propagation on hypergraphs assumes: (i) nodes sharing a hyperedge should exchange more information, and (ii) heavier hyperedges should contribute more to the propagation. With these principles, one layer of hypergraph convolution updates the embedding of node i via

$$\mathbf{x}_i^{(l+1)} = \sigma \left(\sum_{j=1}^N \sum_{\varepsilon=1}^M H_{i\varepsilon} H_{j\varepsilon} W_{\varepsilon\varepsilon} \mathbf{x}_j^{(l)} P^{(l)} \right), \quad (2)$$

where $\mathbf{x}_i^{(l)}$ is the i -th node embedding at layer l , $\sigma(\cdot)$ is a nonlinearity (e.g., LeakyReLU or ELU), and $P^{(l)} \in \mathbb{R}^{F^{(l)} \times F^{(l+1)}}$ is the learnable weight matrix at layer l . In matrix form,

$$X^{(l+1)} = \sigma \left(H W H^\top X^{(l)} P^{(l)} \right),$$

with $X^{(l)} \in \mathbb{R}^{N \times F^{(l)}}$ and $X^{(l+1)} \in \mathbb{R}^{N \times F^{(l+1)}}$.

Normalization. The operator $H W H^\top$ does not control the spectral radius, so stacking many layers can cause scaling issues and unstable optimization. A symmetric normalization yields the normalized propagation

$$X^{(l+1)} = \sigma \left(D^{-\frac{1}{2}} H W B^{-1} H^\top D^{-\frac{1}{2}} X^{(l)} P^{(l)} \right). \quad (3)$$

Here D and B are the degree matrices in (1). One can show the largest eigenvalue of $D^{-\frac{1}{2}} H W B^{-1} H^\top D^{-\frac{1}{2}}$ is at most 1 ensuring stability during optimization.

Node Interaction. Hypergraph convolution respects the neighborhood of each node: a node only aggregates signals from nodes that share at least one hyperedge with it. Let consider

$$H H^\top \in \mathbb{R}^{N \times N}, \quad (H H^\top)_{ij} = \sum_{\varepsilon=1}^M H_{i\varepsilon} H_{j\varepsilon},$$

be the (unweighted) node co-incidence matrix that counts how many hyperedges make v_i and v_j co-incident. The (closed) neighborhood of i is then

$$\mathcal{N}(i) = \{j \in \{1, \dots, N\} : (H H^\top)_{ij} > 0\}.$$

With this notation, the node-wise update in equation (2) can be written as

$$x_i^{(l+1)} = \sigma \left(\sum_{j \in \mathcal{N}(i)} \left(\sum_{\varepsilon=1}^M H_{i\varepsilon} H_{j\varepsilon} W_{\varepsilon\varepsilon} \right) x_j^{(l)} P^{(l)} \right), \quad (4)$$

which makes explicit that only $j \in \mathcal{N}(i)$ contribute to $x_i^{(l+1)}$. In matrix form, the normalized propagation used in equation (3) reads

$$X^{(l+1)} = \sigma \left(S X^{(l)} P^{(l)} \right),$$

$$S := D^{-\frac{1}{2}} H W B^{-1} H^\top D^{-\frac{1}{2}},$$

where S inherits the same sparsity pattern of HH^\top , and thus preserves the neighborhood constraint of equation (4).

Similarly to what happens with graphs, after n layers, a node's representation depends on nodes within n hops in the node–hyperedge incidence, so we define the n -hop neighborhood for node v_i as:

$$\mathcal{N}^n(i) = \{j \in \{1, \dots, N\} : ((HH^\top)^n)_{ij} > 0\}.$$

Model. Since $X^{(l+1)}$ is differentiable w.r.t. both $X^{(l)}$ and $P^{(l)}$, hypergraph convolution layers can be trained end-to-end via gradient-based optimization.

Let $X = X^{(0)} \in \mathbb{R}^{N \times F^{(0)}}$ be the input node features. A hypergraph neural network is obtained by stacking the L convolution layers in (3), producing $X^{(L)}$. A node-level predictor is then defined as

$$\hat{y} = f(H, X, P^{(l)}) := \text{softmax}(X^{(L)}P^{(L)}) \in \mathbb{R}^{N \times C},$$

where $P^{(l)}$, with $l = 0, \dots, L$, collect all learnable parameters. In the following, we will omit the dependency from the learnable parameters P since the counterfactual explanation generation problem assume the model parameters to be frozen. We focus on node classification task: given labeled nodes, the model is trained to predict these labels.

4. Problem Formualtion

4.1. Perturbed Signal Propagation

A convolutional layer on a hypergraph depends on: (i) the structure encoded by the incidence matrix H (which determines the node neighborhood), (ii) the current node embeddings $X^{(l)}$, and (iii) the layer parameters $P^{(l)}$. In analogy with counterfactual sparsification for graphs—where the forward map depends on the adjacency A_v , the local features X_v , and the weights, resulting in $f(A_v, X_v; W)$, and a learnable perturbation P is introduced to obtain a perturbed map $g(A_v, X_v, W; P)$ —we introduce a *learnable perturbation matrix* Π that modulates the neighborhood used by the layer.

Formally, we define a perturbed propagation

$$X^{(l+1)} = \sigma(S(\Pi) X^{(l)} P^{(l)}), \quad (5)$$

where the operator $S(\Pi)$ is obtained by applying the perturbation matrix Π (element-wise, i.e., Hadamard-wise) to the incidence matrix H , thus resulting in:

$$S(\Pi) := D^{-\frac{1}{2}}(H \odot \Pi)WB^{-1}(H \odot \Pi)^\top D^{-\frac{1}{2}}, \quad (6)$$

with the degrees being recomputed whenever the incidence is modified. This mirrors the CF-GNNExplainer's idea of inserting a learnable, differentiable mask into the neighborhood aggregation so that the logits depend on $(H, X^{(l)}, P)$ and on Π .

4.2. Loss Formulation

Similarly to CF-GNNExplainer, we learn Π by solving an optimization problem, where the HGNN parameters are kept fixed and only the mask is optimized.

Optimization Objective. Let f denote the trained HGNN and let $S(\Pi)$ be the perturbed propagation operator introduced in equation (6). Denote by \hat{y} the original predicted label for the explained node under the unperturbed hypergraph, we then learn Π by minimizing the following loss:

$$\mathcal{L}(\Pi) = -\mathcal{L}_{\text{pred}}(f(H \odot \Pi), X), \hat{y} + \beta \mathcal{L}_{\text{dist}}(\Pi), \quad (7)$$

where $-\mathcal{L}_{\text{pred}}$ penalizes the model's confidence in the original class \hat{y} under the perturbed propagation (thus encouraging a prediction change), while $\mathcal{L}_{\text{dist}}$ enforces minimality of the edit and $\beta > 0$ controls the trade-off.

To make equation (7) explicit, we instantiate $\mathcal{L}_{\text{pred}}$ as the log-probability assigned to the original class *prediction* by the perturbed model output so that minimizing $-\mathcal{L}_{\text{pred}}$ the perturbed prediction is pushed away from the original decision without specifying a target class. The regularization term $\mathcal{L}_{\text{dist}}$ is instantiated as the L1 distance between the perturbation matrix and the original incidence matrix. Finally, in direct analogy with CF-GNNExplainer, the prediction term is be made active only while the prediction has not yet flipped by multiplying it by the following term $\mathbb{1}[\arg \max f(H \odot \Pi, X) = \hat{y}]$, with $\mathbb{1}(\cdot)$ being the indicator function.

Continuous Relaxation and Thresholding. Since the incidence matrix H is discrete, the desired perturbation is discrete as well. However, to enable gradient-based optimization, we optimize a continuous relaxation of the mask. Specifically, we learn an continuous perturbation matrix, we map it to $(0, 1)$ via a sigmoid, and use the resulting soft mask in the forward pass. At evaluation time, we obtain an actionable counterfactual hypergraph by thresholding the relaxed mask, using 0.5 as threshold.

4.3. Method Variants

We consider two variants that differ in how the Π is initialized.

(NHP) Node–Hyperedge Perturbation. *Goal: eliminate the participation of a specific node i in selected incident hyperedges ε .*

Let $\pi^{(i)} \in [0, 1]^M$ be a vector of hyperedge-wise learnable perturbation coefficients for node i , and lift it to a rectangular mask $\Pi^{(i)} \in [0, 1]^{N \times M}$ by

$$(\Pi^{(i)})_{k\varepsilon} = \begin{cases} \pi_\varepsilon^{(i)}, & \text{if } k = i, \\ 1, & \text{if } k \neq i. \end{cases}$$

For any neighbor j that communicates with i through a hyperedge ε , the message from j to i now carries a factor $\pi_\varepsilon^{(i)}$ (since $H'_{i\varepsilon} = \pi_\varepsilon^{(i)} H_{i\varepsilon}$ while $H'_{j\varepsilon} = H_{j\varepsilon}$), so that setting $\pi_\varepsilon^{(i)} \approx 0$ softly (or, in the binary case, hard-) removes the contribution carried through ε to the representation of v_i without altering the incidences of other nodes.

(HP) Hyperedge Perturbation. *Goal: eliminate entire hyperedges in the local neighborhood of a target node v_i .* Let $\Pi \in [0, 1]^{N \times M}$ be row-constant and tunable only in the n -hop neighborhood of v_i , i.e.,

$$\forall k = 1, \dots, N \quad (\Pi^{(i)})_{k\varepsilon} = \begin{cases} \pi_\varepsilon, & \text{if } \varepsilon \in \mathcal{N}^n(i), \\ 1, & \text{if } \varepsilon \notin \mathcal{N}^n(i). \end{cases}$$

For every hyperedge $\varepsilon \in \mathcal{N}^n(i)$ and every incident node k to it we have $H'_{k\varepsilon} = \pi_\varepsilon H_{k\varepsilon}$, while hyperedges outside $\mathcal{N}^n(i)$ are unchanged. Hence, any message that traverses a hyperedge ε within the n -hop computation around v_i is uniformly scaled by π_ε (note that ε need not be incident to v_i , it only needs to lie on an information-flow path in $\mathcal{N}^n(i)$). Setting $\pi_\varepsilon \approx 0$ therefore suppresses all interactions mediated by ε in that neighborhood, effectively removing the corresponding conduit of information flow for all nodes participating in ε .

Remarks. All variants plug into equation (5) by treating the perturbation as a differentiable mask over the neighborhood structure. When the incidence matrix is modified (NHP, HP), we recompute the induced node and hyperedge degrees so that normalization remains consistent with the perturbed connectivity. The two variants offer complementary control: (HP) provides hyperedge-level gating, while (NHP) enables finer node-hyperedge edits, allowing different granularities of counterfactual neighborhood intervention.

5. Experimental Setup

5.1. Implementation Details

We run all experiments on a machine equipped with an AMD Ryzen 9 7900 12-Core Processor and an NVIDIA GeForce RTX 4090 GPU. Our implementation is based on the PyTorch Geometric framework. We implemented both variants of the method using dense matrices, similarly to CF-GNNExplainer (Lucic et al., 2022), denoted with CF-HyperGNNExplainer_{dense}.

To further improve the speed of our method, we implemented a version designed for sparse matrices using the COO format, denoted with CF-HyperGNNExplainer_{sparse}. The COO format stores only the non-zero elements of a matrix along with their coordinates, which is particularly

efficient for the hypergraph incidence matrices, which are typically very sparse. This version is designed to be faster and more memory-efficient, compared to the traditional dense version. The code is publicly available on GitHub¹.

5.2. Datasets and Models

To assess the performance of CF-HyperGNNExplainer, we used three widely-used citation network datasets proposed by Yang et al. (Yang et al., 2016): Cora, CiteSeer, and PubMed. In all the three datasets, nodes represent scientific papers, edges represent citations, and node features are extracted using a bag-of-words approach with a fixed vocabulary.

Cora and CiteSeer share similar dimensionality, with nearly 3,000 nodes and 10,000 edges, but differ in the number of features (1,433 and 3,703, respectively) and classes (7 and 6, respectively). PubMed is significantly larger, containing nearly 20,000 nodes, 90,000 edges, 500 features, and 3 classes. For all the datasets, we used the train/validation/test splits defined by Yang et al. (Yang et al., 2016).

Since these datasets are originally standard graphs, we converted them to hypergraphs using a neighborhood-based conversion, which is well suited for citation networks. For each node i in the graph, we define a hyperedge ε_i that contains node i and all its neighbors. This results in a hypergraph with N nodes and N hyperedges.

The model used in all the experiments is a 3-layer Hypergraph Convolutional Network inspired by the architecture of the one used by Lucic et al. (Lucic et al., 2022), with hidden dimensions of 64 and 32, Leaky ReLU activation function, a dropout probability of 0.5 used during training, and a final linear classification layer. The model was trained for 200 epochs using a learning rate of 0.01, a weight decay of 5×10^{-4} and SGD as optimizer.

5.3. Baselines

We compared CF-HyperGNNExplainer against two state-of-the-art counterfactual explainers for GNNs: CF-GNNExplainer (Lucic et al., 2022) and RCEExplainer (Bajaj et al., 2022). Since both methods are designed for standard graphs rather than hypergraphs, we evaluated them in two different settings, to ensure a fair comparison with our method.

We tested both baselines on the original Cora graph to assess their performance on a traditional graph. To perform a direct comparison with our hypergraph-based method, we converted the Cora hypergraph back to a standard graph using star expansion. This step is necessary to evaluate

¹<https://anonymous.4open.science/r/CF-HyperGNNExplainer-0716>

how our method performs when the dataset is natively a hypergraph, where the alternatives are either using our hypergraph method directly or converting to a graph and then applying graph-native methods. In star expansion, each hyperedge ϵ is replaced by an auxiliary node v_ϵ , and all the nodes incident to the hyperedge are connected to v_ϵ . While this transformation preserves the hypergraph's higher-order information, it produces a substantially larger graph. Specifically, in our case, the resulting graph has $N + N = 2N$ nodes, and its adjacency matrix has size $2N \times 2N$, four times larger than the hypergraph representation.

5.4. Metrics

For each node in the test split V_{test} of the graph, we generated a CF example and evaluated the performance of CF-HyperGNExplainer using three metrics.

Accuracy: is defined as the proportion of nodes for which the explainer successfully finds a valid CF example. Formally:

$$\text{Accuracy} = \frac{1}{|V_{\text{test}}|} \sum_{v \in V_{\text{test}}} \mathbb{1}[\exists H' : f_v(H', X) \neq f_v(H, X)]$$

where $f_v(H, X)$ denotes the model's prediction for the node v on the original hypergraph and $f_v(H', X)$ denotes the prediction for the node v on the CF hypergraph.

Explanation Size: measures the amount of structural change required to obtain a CF example. The definition differs depending on the method's variant. For variant NHP, is measured as the number of node-hyperedge incidences removed from the original incidence matrix H for the node we are considering. For variant HP, the explanation size is measured as the number of hyperedges removed from H . Formally, the metric for variant NHP is:

$$\text{Size}_{\text{NHP}}(H, H') = \sum_{i=1}^N \sum_{\epsilon=1}^M |H_{i\epsilon} - H'_{i\epsilon}|$$

while, the metric for variant HP is:

$$\text{Size}_{\text{HP}} = \sum_{\epsilon \in \mathcal{E}} \mathbb{1}[\epsilon \notin \mathcal{E}_{\text{cf}}]$$

where \mathcal{E} is the set of hyperedges in the original hypergraph and \mathcal{E}_{cf} is the set of hyperedges in the CF hypergraph.

Sparsity: measures the fraction of the original hypergraph structure preserved in the CF explanation. For variant NHP, it is defined as the fraction of incidences that are preserved in the CF hypergraph's incidence matrix H . Formally:

$$\text{Sparsity}_{\text{NHP}} = 1 - \frac{\text{Size}_{\text{NHP}}}{\sum_{i,\epsilon} H_{i\epsilon}}$$

For variant HP, sparsity is defined as the fraction of hyperedges preserved. Formally:

$$\text{Sparsity}_{\text{HP}} = 1 - \frac{\text{Size}_{\text{HP}}}{|\mathcal{E}|}$$

5.5. Hyperparameter Search

We measured the effect of different optimization hyperparameters for CF-HyperGNExplainer, focusing on learning rate and the momentum term of the SGD optimizer. In particular, we tested learning rates $\alpha \in \{0.1, 0.01\}$ and momentum values $m \in \{0, 0.5, 0.9\}$ on the Cora dataset. The results are reported in Tables 3 and 4.

Across both variants of the method, higher learning rates and momentum consistently resulted in higher accuracy (i.e., a larger number of valid CF examples). Based on this results, we used a learning rate of $\alpha = 0.1$ and a momentum of $m = 0.9$ in all experiments.

6. Results

In this section, we present an evaluation of CF-HyperGNExplainer on multiple benchmark datasets. We first assess its performance on citation network hypergraphs, considering both proposed method's variants. We then compare our approach with existing graph-based CF explanation methods and provide an ablation study to analyze the impact of key optimization hyperparameters.

6.1. Performance on Citation Networks

Table 1 illustrates the performance of CF-HyperGNExplainer across the three citation network datasets using both the incidence-level (NHP) and hyperedge-level (HP) method variants.

Both variants successfully generated CF explanations across all datasets. The NHP variant produced valid counterfactuals for 72.0% of the test nodes on Cora, 72.7% in CiteSeer, and 50.6% on PubMed. The HP variant produced valid counterfactuals for 64.7% of the test nodes on Cora, 61.3% on CiteSeer, and 52.4% on PubMed. Both variants achieved lower accuracy on PubMed compared to Cora and CiteSeer, likely due to the dataset's larger scale and sparsity.

Both variants produced highly sparse explanations, preserving most of the original hypergraph structure. For the NHP variant, sparsity varies from 89.4% on CiteSeer to 99.9% on PubMed, with an average explanation size of 2.5-2.9 incidence removals. For the HP variant, the sparsity values are similar, varying from 89.9% on CiteSeer to 99.9% on PubMed, with an average explanation size of 2.9-3.2 hyperedge removals.

6.2. Comparison with Graph-Based Methods

Table 2 shows the performance difference between CF-HyperGNNEExplainer and the graph-based baselines on the Cora dataset. CF-HyperGNNEExplainer achieved the highest accuracy (72.0%) among all methods, outperforming both CF-GNNExplainer and RCEExplainer in both settings: the original graph, and the one obtained using star-expansion. This result demonstrates that our hypergraph-native approach is more effective at producing valid counterfactual explanations than adapting graph-based methods to hypergraphs. In terms of sparsity, CF-HyperGNNEExplainer (98.2%) and CF-GNNExplainer (96.3% on the original graph, 97.5% on the star-expanded graph) both produced highly sparse explanations that preserve most of the original structure. In contrast, RCEExplainer generated significantly less sparse explanations (22.2% on the original graph, 25.5% on the star-expanded graph), with significantly larger explanation sizes (7.8 and 19.7 incidence changes, respectively). This suggests that RCEExplainer requires larger modification to the graph’s structure to generate a counterfactual explanation.

Table 5 reports the average time taken to generate a counterfactual explanation for each method. The sparse implementation of CF-HyperGNNEExplainer is significantly faster than CF-GNNExplainer, with a speedup of 13.5x for the NHP variant and 13.9x for the HP variant. While RCEExplainer is significantly faster than CF-GNNExplainer, it is still slower compared to the sparse implementations of CF-HyperGNNEExplainer.

These results highlight that CF-HyperGNNEExplainer not only generates high quality counterfactual explanations, but is also significantly faster and more efficient than the graph-based methods.

7. Limitations

Sparse Hypergraphs. The NHP variant works by removing node-hyperedge incidences. For a node v with degree d_v , there exist 2^{d_v} possible combinations of incidences that can be kept or removed. When d_v is small enough, exhaustive enumeration of all possible combinations becomes feasible

and more efficient than the proposed method.

This limitation is specific to the NHP variant, due to the node-centric perturbation strategy. The HP strategy, which operates on hyperedges within n -hop neighborhood, typically generates a larger search space and therefore benefits more from gradient-based optimization.

Random Baseline Performance and Theoretical Lower Bound.

Random perturbation baselines are able to find a large number of valid counterfactuals, but typically generate explanations with significantly larger explanation sizes compared to the gradient-based approaches. However, for the NHP variant in very sparse hypergraphs, there exists a lower bound on the probability of randomly discovering the smallest counterfactual.

Assume that the smallest counterfactual exists and is unique. For a target node v with degree d_v , the probability of randomly obtaining the minimal counterfactual in t independent sampling attempts, where each incidence is kept or removed with probability $\frac{1}{2}$, is given by:

$$P(d_v, t) = 1 - \left(1 - \left(\frac{1}{2}\right)^{d_v}\right)^t \quad (8)$$

This probability follows from the theory of Bernoulli trials, where each sampling attempt represents an independent trial with success probability $(\frac{1}{2})^{d_v}$. It is important to note that equation (8) represents a theoretical lower bound on the probability, as in practice there may exist multiple counterfactuals at the same minimal distance from the original sample.

This lower bound demonstrates that in very sparse hypergraphs, the probability of randomly generating the minimal counterfactual becomes significantly high, even with a small number of sampling attempts. For example, with $d_v = 5$ and $t = 100$ attempts, the probability exceeds 0.95.

8. Conclusions and Future Work

In this work, we introduced CF-HyperGNNEExplainer, the first counterfactual explanation method specifically designed for Hypergraph Neural Networks. Our approach

Table 1. Performance of NHP and HP Method Variants on Cora, CiteSeer and PubMed datasets. The values for *Sparsity* and *Explanation Size* are calculated as the average of the entire test set, with \pm standard deviation.

Method	Dataset	Variant	Accuracy \uparrow	Sparsity \uparrow	Explanation Size \downarrow
CF-HyperGNNEExplainer	Cora	NHP	0.720	0.982 ± 0.084	2.917 ± 1.487
CF-HyperGNNEExplainer	CiteSeer	NHP	0.727	0.894 ± 0.178	2.667 ± 1.423
CF-HyperGNNEExplainer	PubMed	NHP	0.506	$0.999 \pm 1.631 \times 10^{-5}$	2.488 ± 1.691
CF-HyperGNNEExplainer	Cora	HP	0.647	0.986 ± 0.078	3.202 ± 3.262
CF-HyperGNNEExplainer	CiteSeer	HP	0.613	0.899 ± 0.206	3.052 ± 2.818
CF-HyperGNNEExplainer	PubMed	HP	0.524	$0.999 \pm 1.334 \times 10^{-4}$	2.863 ± 2.601

generates counterfactual explanations by performing minimal edits to the hypergraph incidence matrix, either by removing node-hyperedge incidences (NHP variant) or by removing entire hyperedges (HP variant).

Experimental results on three citation network datasets demonstrate that CF-HyperGNNEExplainer successfully generates valid and concise counterfactual explanations. Both method variants achieve high accuracy (up to 72.7% on CiteSeer), while maintaining high sparsity, indicating that only minimal changes are required to alter the model prediction. We then compared our method to existing state-of-the-art counterfactual explainers for graphs, demonstrating that CF-HyperGNNEExplainer outperforms these approaches both in terms of the number of valid counterfactuals found and

explanation quality. Moreover, our sparse implementation achieves significant computational efficiency gains, with speedups of up to 13.9x compared to graph-based models.

Both variants of CF-HyperGNNEExplainer are currently restricted to deletion operations on the incidence matrix and are designed for node classification. Future work will broaden the set of allowable interventions to generate richer counterfactuals, including perturbations of node features and the addition of incidences or hyperedges. Another promising direction is to extend the method to hypergraph-level prediction tasks (hypergraph classification), which, while less common than node classification, are increasingly relevant in several application domains.

Table 2. Performance comparison of CF-HyperGNNEExplainer NHP variant and CF-GNNEExplainer methods. The * denotes the variants operating on the graph obtained from the hypergraph using star expansion.

Method	Dataset	Variant	Accuracy \uparrow	Sparsity \uparrow	Explanation Size \downarrow
CF-HyperGNNEExplainer (ours)	Cora	NHP	0.720	0.982 \pm 0.084	2.917 \pm 1.487
CF-GNNEExplainer*	Cora	N/A	0.497	0.975 \pm 0.088	3.044 \pm 2.687
CF-GNNEExplainer	Cora	N/A	0.499	0.963 \pm 0.151	2.379 \pm 1.913
RCEExplainer*	Cora	N/A	0.575	0.255 \pm 0.383	19.743 \pm 18.149
RCEExplainer	Cora	N/A	0.410	0.222 \pm 0.363	7.800 \pm 16.424

Table 3. Performance comparison between the NHP and HP strategies using different learning rates using the Cora Dataset. A lower learning rate enables the generation of smaller counterfactual samples, but reduces the number of samples found in the test set.

Learning Rate	Variant	Accuracy \uparrow	Sparsity \uparrow	Explanation Size \downarrow
0.1	NHP	0.720	0.982 \pm 0.084	2.917 \pm 1.487
0.01	NHP	0.453	0.983 \pm 0.084	2.188 \pm 1.081
0.1	HP	0.647	0.986 \pm 0.078	3.202 \pm 3.262
0.01	HP	0.385	0.989 \pm 0.071	1.969 \pm 1.006

Table 4. Performance comparison between the NHP and HP strategies using different momentum values for SGD, using the Cora Dataset.

Momentum	Variant	Accuracy \uparrow	Sparsity \uparrow	Explanation Size \downarrow
0.9	NHP	0.720	0.982 \pm 0.084	2.917 \pm 1.487
0.5	NHP	0.464	0.979 \pm 0.094	2.205 \pm 1.104
0	NHP	0.454	0.983 \pm 0.084	2.187 \pm 1.084
0.9	HP	0.647	0.986 \pm 0.078	3.202 \pm 3.262
0.5	HP	0.388	0.996 \pm 0.036	1.884 \pm 0.963
0	HP	0.309	0.996 \pm 0.041	1.583 \pm 0.713

Table 5. Average time to generate a CF explanation between CF-HyperGNNEExplainer and the graph-based methods (in seconds).

Method	Dataset	Variant	Explanation Time	Speedup
CF-HyperGNNEExplainer _{dense} (ours)	Cora	NHP	19.630	2.3x
CF-HyperGNNEExplainer _{sparse} (ours)	Cora	NHP	3.299	13.5x
CF-HyperGNNEExplainer _{dense} (ours)	Cora	HP	6.282	7.1x
CF-HyperGNNEExplainer _{sparse} (ours)	Cora	HP	3.190	13.9x
CF-GNNEExplainer*	Cora	N/A	44.449	1.0x
RCEExplainer*	Cora	N/A	4.891	9.1x

References

an Bi, X., Luo, S., Jiang, S., Wang, Y., Xing, Z., and Xu, L. Explainable and programmable hypergraph convolutional network for imaging genetics data fusion. *Information Fusion*, 100:101950, 2023. ISSN 1566-2535. doi: <https://doi.org/10.1016/j.inffus.2023.101950>. URL <https://www.sciencedirect.com/science/article/pii/S156625352300266X>.

Bajaj, M., Chu, L., Xue, Z. Y., Pei, J., Wang, L., Lam, P. C.-H., and Zhang, Y. Robust counterfactual explanations on graph neural networks, 2022. URL <https://arxiv.org/abs/2107.04086>.

Battiston, F., Cencetti, G., Iacopini, I., Latora, V., Lucas, M., Patania, A., Young, J., and Petri, G. Networks beyond pairwise interactions: Structure and dynamics. *Physics Reports*, 874:1–92, August 2020. ISSN 0370-1573. doi: 10.1016/j.physrep.2020.05.004. Publisher Copyright: © 2020 The Authors.

Feng, Y., You, H., Zhang, Z., Ji, R., and Gao, Y. Hypergraph neural networks. In *Proceedings of the Thirty-Third AAAI Conference on Artificial Intelligence and Thirty-First Innovative Applications of Artificial Intelligence Conference and Ninth AAAI Symposium on Educational Advances in Artificial Intelligence, AAAI’19/IAAI’19/EAAI’19*. AAAI Press, 2019. ISBN 978-1-57735-809-1. doi: 10.1609/aaai.v33i01.33013558. URL <https://doi.org/10.1609/aaai.v33i01.33013558>.

Kim, S., Lee, S. Y., Gao, Y., Antelmi, A., Polato, M., and Shin, K. A survey on hypergraph neural networks: An in-depth and step-by-step guide. In *Proceedings of the 30th ACM SIGKDD Conference on Knowledge Discovery and Data Mining*, KDD ’24, pp. 6534–6544, New York, NY, USA, 2024. Association for Computing Machinery. ISBN 9798400704901. doi: 10.1145/3637528.3671457. URL <https://doi.org/10.1145/3637528.3671457>.

Lucic, A., Ter Hoeve, M. A., Tolomei, G., De Rijke, M., and Silvestri, F. Cf-gnnexplainer: Counterfactual explanations for graph neural networks. In Camps-Valls, G., Ruiz, F. J. R., and Valera, I. (eds.), *Proceedings of The 25th International Conference on Artificial Intelligence and Statistics*, volume 151 of *Proceedings of Machine Learning Research*, pp. 4499–4511. PMLR, 28–30 Mar 2022. URL <https://proceedings.mlr.press/v151/lucic22a.html>.

Luo, D., Cheng, W., Xu, D., Yu, W., Zong, B., Chen, H., and Zhang, X. Parameterized explainer for graph neural network. In Larochelle, H., Ranzato, M., Hadsell, R., Balcan, M., and Lin, H. (eds.), *Advances in Neural Information Processing Systems*, volume 33, pp. 19620–19631. Curran Associates, Inc., 2020. URL https://proceedings.neurips.cc/paper_files/paper/2020/file/e37b08dd3015330dcbb5d6663667b8b8-Paper.pdf.

Maleki, S., Hajiramezalani, E., Scalia, G., Biancalani, T., and Chuang, K. V. Learning to explain hypergraph neural networks. URL <https://api.semanticscholar.org/CorpusID:271910080>.

Su, S., Duta, I., Magister, L. C., and Liò, P. Explaining hypergraph neural networks: From local explanations to global concepts, 2024. URL <https://arxiv.org/abs/2410.07764>.

Wachter, S., Mittelstadt, B., and Russell, C. Counterfactual Explanations without Opening the Black Box: Automated Decisions and the GDPR. *Harvard Journal of Law & Technology.*, 31:841–887, 2017.

Yadati, N., Nimishakavi, M., Yadav, P., Nitin, V., Louis, A., and Talukdar, P. *HyperGCN: a new method of training graph convolutional networks on hypergraphs*. Curran Associates Inc., Red Hook, NY, USA, 2019.

Yang, Z., Cohen, W. W., and Salakhutdinov, R. Revisiting semi-supervised learning with graph embeddings, 2016. URL <https://arxiv.org/abs/1603.08861>.

Ying, R., Bourgeois, D., You, J., Zitnik, M., and Leskovec, J. *GNNEExplainer: generating explanations for graph neural networks*. Curran Associates Inc., Red Hook, NY, USA, 2019.

Yu, L., Cai, Y., Zhang, M., and Hu, X. Self-explaining hypergraph neural networks for diagnosis prediction. In Xu, X. O., Choi, E., Singhal, P., Gerych, W., Tang, S., Agrawal, M., Subbaswamy, A., Sizikova, E., Dunn, J., Daneshjou, R., Sarker, T., McDermott, M., and Chen, I. (eds.), *Proceedings of the sixth Conference on Health, Inference, and Learning*, volume 287 of *Proceedings of Machine Learning Research*, pp. 908–924. PMLR, 25–27 Jun 2025. URL <https://proceedings.mlr.press/v287/yu25a.html>.

Zhou, D., Huang, J., and Schölkopf, B. Learning with hypergraphs: Clustering, classification, and embedding. In Schölkopf, B., Platt, J., and Hoffman, T. (eds.), *Advances in Neural Information Processing Systems*, volume 19. MIT Press, 2006. URL https://proceedings.neurips.cc/paper_files/paper/2006/file/dff8e9c2ac33381546d96deea9922999-Paper.pdf.